

# Homodyne detection for the enhancement of antibunching

Reeta Vyas, Changxin Wang, and Surendra Singh

*Physics Department, University of Arkansas, Fayetteville, AR 72701*

(Received 15 February 1996; revised manuscript received 22 April 1996)

We propose a scheme based on homodyne detection for enhancing antibunching in second-harmonic generation and multiatom optical bistability. We show that depending on the reflectivity of the beam splitter, relative field strengths, and relative phase it is possible to achieve perfect antibunching in the superposed field. We also discuss other nonclassical effects exhibited by the superposed field and present curves to illustrate the behavior. [S1050-2947(96)09008-7]

PACS number(s): 42.50.Dv, 42.50.Ar, 42.65.Ky

## I. INTRODUCTION

Squeezing [1], antibunching, and sub-Poissonian statistics [2,3] are nonclassical features of the electromagnetic field. These nonclassical features have been of considerable interest as they provide testing grounds for the prediction of quantum electrodynamics. Squeezing is related to the wavelike character of the electromagnetic field. It is measured in interference experiments. Antibunching and sub-Poissonian statistics, however, reflect the particlelike behavior of the field and are measured in photon counting experiments. As discussed in Ref. [4] squeezing, antibunching, and sub-Poissonian statistics are, in general, distinct nonclassical effects in the sense that an electromagnetic field may exhibit one but not the other.

The antibunching effect has been predicted in intracavity second-harmonic generation (ISHG) [5,6] and multiatom optical bistability (MAOB) [7,8]. However, the predicted size of antibunching is small and would be difficult to detect experimentally, as it occurs against a large coherent background. The predicted antibunching in these systems is inversely proportional to the saturation photon number  $n_{\circ}$ , which is of the order of  $10^6-10^8$  for the ISHG, and  $10^3-10^4$  for the MAOB. Several schemes based on interference [9] or passive filter cavities [10-12] have been proposed to enhance the antibunching effect.

We propose a scheme based on homodyne detection [13-15] for enhancing antibunching in these systems. Homodyne detection experiments have been used for measuring phase-sensitive properties of squeezed light [1]. It has been shown that the light from a degenerate parametric oscillator, which is highly bunched and super-Poissonian [16,17], can exhibit many nonclassical effects using a similar detection scheme [13]. In the homodyne detection experiment we consider the interference of the signal beam from the ISHG or the MAOB with a coherent local oscillator (LO) at a lossless beam splitter as shown in Fig. 1. A detector of efficiency  $\eta$  is placed at one of the output ports of the beam splitter. The statistics measured at the detector is sensitive to the relative phase between the signal and the LO. Thus particlelike properties (photon statistics) are intimately connected to wavelike (phase) property of the field. Because of this phase dependence, the homodyne field can exhibit enhanced antibunching and violation of various classical inequalities. Since in this scheme one can readily adjust various parameters such

as the strength of the local oscillator, transmittance, and relative phase, this scheme may provide a better way of enhancing antibunching.

In Sec. II we briefly describe the homodyne detection scheme. In Sec. III we apply this technique to the ISHG. In Sec. IV we discuss the enhancement of antibunching for the MAOB. Finally, a summary and main conclusions of the paper are presented in Sec. V.

## II. HOMODYNE DETECTION

Figure 1 shows a schematic diagram for the homodyne detection experiment. For the ISHG, a nonlinear crystal is placed inside the cavity, whereas for the MAOB,  $N$  two-level atoms are placed inside the cavity. The light from the ISHG or the MAOB is superimposed with the light from a LO at a lossless beam splitter. The annihilation operators  $\hat{b}_1$  and  $\hat{b}_2$  at the output ports are related to those at the input ports by [13,14]

$$\begin{pmatrix} \hat{b}_1 \\ \hat{b}_2 \end{pmatrix} = \begin{pmatrix} \sqrt{T} & \sqrt{R} \\ -\sqrt{R} & \sqrt{T} \end{pmatrix} \begin{pmatrix} \hat{a}_s \\ \hat{a}_l \end{pmatrix},$$

with

$$T + R = 1.$$

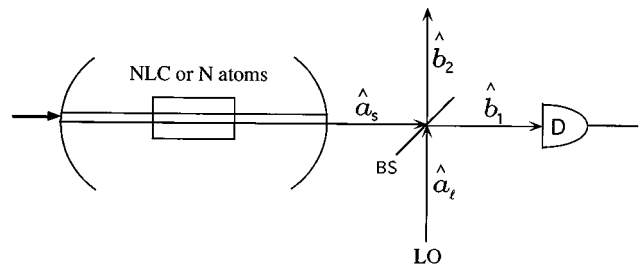


FIG. 1. System for homodyning the ISHG or MAOB field with the LO field. For the ISHG a nonlinear crystal (NLC) is placed inside the cavity and for the MAOB  $N$  two-level atoms are placed inside the cavity. BS denotes a beam splitter and  $D$  denotes a detector.

Here  $\hat{a}_s$  and  $\hat{a}_\ell$  are annihilation operators for the signal and the local oscillator, respectively,  $\mathcal{T}$  is the transmissivity, and  $\mathcal{R}$  is the reflectivity of the beam splitter. For  $\mathcal{T}=1$  only the light from the signal is detected, and for  $\mathcal{T}=0$  only the light from the LO is detected. Here we assume that the fields suffer no phase shifts due to the beam splitter. We will refer the superposed field as HISHG when the signal is from the ISHG and as HMAOB when the signal is from the MAOB.

The annihilation and creation operators at the ‘‘sum’’ output port  $\hat{b}_1$  can be written as

$$\hat{b}_1 = \hat{a}_s \sqrt{\mathcal{T}} + \hat{a}_\ell \sqrt{\mathcal{R}}, \quad \hat{b}_1^\dagger = \hat{a}_s^\dagger \sqrt{\mathcal{T}} + \hat{a}_\ell^\dagger \sqrt{\mathcal{R}}. \quad (1)$$

Results for the ‘‘difference’’ port  $\hat{b}_2$  can be obtained by replacing  $\sqrt{\mathcal{T}}$  by  $-\sqrt{\mathcal{R}}$  and  $\sqrt{\mathcal{R}}$  by  $\sqrt{\mathcal{T}}$ .

In the photoelectric counting measurements we are dealing with normally ordered operator expectation values. We can therefore use the positive- $P$  representation to describe the nonclassical fields generated in the ISHG or the MAOB. In the positive- $P$  representation [18], complex-field amplitudes  $\beta_1$  and  $\beta_{1*}$  corresponding to  $\hat{b}_1$  and  $\hat{b}_1^\dagger$  can be written as

$$\beta_1 = \alpha_s \sqrt{\mathcal{T}} + |\alpha_\ell| e^{i\phi} \sqrt{\mathcal{R}}, \quad (2)$$

$$\beta_{1*} = \alpha_{s*} \sqrt{\mathcal{T}} + |\alpha_\ell| e^{-i\phi} \sqrt{\mathcal{R}}. \quad (3)$$

Here  $|\alpha_\ell|$  is the field amplitude for the LO field;  $\phi$  is the LO phase relative to the signal;  $\alpha_s$  and  $\alpha_{s*}$  are the complex-field amplitudes corresponding to  $\hat{a}_s$  and  $\hat{a}_s^\dagger$  for the signal field. Note that in the positive- $P$  representation  $\alpha_s$  and  $\alpha_{s*}$  are not complex conjugates of each other. The mean photon number measured at the detector is proportional to

$$\langle \beta_{1*} \beta_1 \rangle = \mathcal{T} \langle \alpha_{s*} \alpha_s \rangle + \mathcal{R} |\alpha_\ell|^2 + \sqrt{\mathcal{R}} \sqrt{\mathcal{T}} |\alpha_\ell| (\langle \alpha_s \rangle e^{-i\phi} + \langle \alpha_{s*} \rangle e^{i\phi}), \quad (4)$$

and the two-time intensity correlation function can be written as

$$g^{(2)}(T) = \frac{\langle \beta_{1*}(0) \beta_{1*}(T) \beta_1(T) \beta_1(0) \rangle}{\langle \beta_{1*}(0) \beta_1(0) \rangle^2}. \quad (5)$$

Once the correlations properties of  $\alpha_s$  and  $\alpha_{s*}$  are known we can calculate the two-time intensity correlation function. In the literature, antibunching is defined [2–4,19,20] either as a violation of inequality  $g^{(2)}(0) \geq 1$  or inequality  $g^{(2)}(0) \geq g^{(2)}(T)$ . As discussed in Ref. [13] we consider a photon sequence antibunched if the probability of detecting two photons in coincidence is smaller than that for coherent light; that is,  $g^{(2)}(0) < 1$ .

### III. INTRACAVITY SECOND-HARMONIC GENERATION

First consider the light from the ISHG. In the process of second-harmonic generation two photons at the fundamental frequency  $\omega$  combine to give a single photon at the second-harmonic frequency  $2\omega$  inside a nonlinear crystal. The generation of second-harmonic light is enhanced by placing the nonlinear crystal inside an optical cavity that is resonant at

both the fundamental and the second-harmonic frequencies. The fundamental mode of the cavity is excited by an injected classical signal of normalized amplitude  $E$ , which has been chosen to be real by an appropriate definition of phases. This source is known to produce an antibunched photon sequence [5,6].

In the positive- $P$  representation [18] the equations of motion for the complex-field amplitudes  $\alpha_s$  and  $\alpha_{s*}$  associated with the annihilation and creation operators [6,10,11] of the fundamental mode can be written as

$$\dot{\alpha}_s = -\gamma(\alpha_s - E) - \frac{k^2}{2\gamma_2} \alpha_{s*} \alpha_s^2 + i \sqrt{\frac{k^2}{2\gamma_2}} \alpha_s \xi, \quad (6)$$

$$\dot{\alpha}_{s*} = -\gamma(\alpha_{s*} - E) - \frac{k^2}{2\gamma_2} \alpha_{s*}^2 \alpha_s + i \sqrt{\frac{k^2}{2\gamma_2}} \alpha_{s*} \xi_*. \quad (7)$$

Here  $\gamma_1 = \gamma$  and  $\gamma_2$  are the cavity linewidths at the fundamental and its second-harmonic frequencies, and  $k$  is the mode-coupling constant. Noise sources  $\xi$  and  $\xi_*$  are two real Gaussian white-noise processes with zero mean and unit strength [21,22]. These equations of motion are derived by adiabatically eliminating the second harmonic mode ( $\gamma_2 \gg \gamma$ ). By linearizing  $\alpha_s$  and  $\alpha_{s*}$  around the steady-state value  $\bar{n}$  and introducing new variables  $u_1$  and  $u_2$  by

$$\alpha_s = \sqrt{\bar{n}_o} [\sqrt{\bar{n}} + i(u_1 + u_2)], \quad (8)$$

$$\alpha_{s*} = \sqrt{\bar{n}_o} [\sqrt{\bar{n}} + i(u_1 - u_2)], \quad (9)$$

we can show that  $u_1$  and  $u_2$  satisfy the following stochastic differential equations:

$$\dot{u}_i = -\lambda_i u_i + \sqrt{\frac{\gamma \bar{n}}{2n_o}} q_i, \quad i=1,2. \quad (10)$$

Here the threshold photon number  $n_o = 2\gamma\gamma_2/k^2$ ; the average photon number  $\bar{n}$  in the fundamental mode is given by the equation  $(1+\bar{n})^2 \bar{n} n_o = E^2$ ;  $q_1 = (\xi + \xi_*)/\sqrt{2}$  and  $q_2 = (\xi - \xi_*)/\sqrt{2}$  are two real independent Gaussian white-noise processes with zero mean and unit strength. The equation for  $\bar{n}$  has only one physical root. The decay constants  $\lambda_1$  and  $\lambda_2$  are given by

$$\lambda_1 = \gamma(1+3\bar{n}), \quad \lambda_2 = \gamma(1+\bar{n}). \quad (11)$$

It follows from Eq. (10) that  $u_1$  and  $u_2$  are real Gaussian random variables with mean  $\langle u_i \rangle = 0$  and correlations given by

$$\langle u_i(t) u_j(t') \rangle = \delta_{ij} \frac{\gamma \bar{n}}{4n_o \lambda_i} e^{-\lambda_i |t-t'|}, \quad i=1,2. \quad (12)$$

Substituting  $\alpha_s$  and  $\alpha_{s*}$  given by Eqs. (8) and (9) in Eqs. (2) and (3) we get the complex-field amplitudes for the HISHG as

$$\beta_1 = \sqrt{\bar{n}_o} [\sqrt{\bar{n}} + i(u_1 + u_2)] \sqrt{\mathcal{T}} + |\alpha_\ell| e^{i\phi} \sqrt{\mathcal{R}}, \quad (13)$$

$$\beta_{1*} = \sqrt{\bar{n}_o} [\sqrt{\bar{n}} + i(u_1 - u_2)] \sqrt{\mathcal{T}} + |\alpha_\ell| e^{-i\phi} \sqrt{\mathcal{R}}. \quad (14)$$

Using the correlation properties of  $u_1$  and  $u_2$  given in Eq. (12) we obtain the mean for the HISHG as

$$\begin{aligned} \langle \beta_{1*} \beta_1 \rangle &= [\langle \alpha_{s*} \alpha_s \rangle T + |\alpha_r|^2 \mathcal{R}], \\ &= n_o \left[ A + \mathcal{T} \left\{ \left( \frac{\gamma \bar{n}}{4n_o \lambda_2} \right) - \left( \frac{\gamma \bar{n}}{4n_o \lambda_1} \right) \right\} \right]. \end{aligned} \quad (15)$$

The two-time intensity correlation function for the HISHG is similarly given by

$$\begin{aligned} g^{(2)}(T) &= 1 + \frac{\left[ 2T^2 \left\{ \left( \frac{\gamma \bar{n}}{4n_o \lambda_1} \right)^2 e^{-2\lambda_1 T} + \left( \frac{\gamma \bar{n}}{4n_o \lambda_2} \right)^2 e^{-2\lambda_2 T} \right\} \right]}{\left[ A + \mathcal{T} \left\{ \left( \frac{\gamma \bar{n}}{4n_o \lambda_2} \right) - \left( \frac{\gamma \bar{n}}{4n_o \lambda_1} \right) \right\} \right]^2} \\ &+ \frac{\left[ -C^2 \left( \frac{\gamma \bar{n}}{4n_o \lambda_1} \right) e^{-\lambda_1 T} + D^2 \left( \frac{\gamma \bar{n}}{4n_o \lambda_2} \right) e^{-\lambda_2 T} \right]}{\left[ A + \mathcal{T} \left\{ \left( \frac{\gamma \bar{n}}{4n_o \lambda_2} \right) - \left( \frac{\gamma \bar{n}}{4n_o \lambda_1} \right) \right\} \right]^2}, \end{aligned} \quad (16)$$

where

$$A = \bar{n} T + \bar{n}_r \mathcal{R} + 2\sqrt{\bar{n}} \sqrt{\bar{n}_r} \sqrt{\mathcal{T}} \sqrt{\mathcal{R}} \cos(\phi), \quad (17)$$

$$C = 2[\sqrt{\bar{n}} T + \sqrt{\bar{n}_r} \sqrt{\mathcal{T}} \sqrt{\mathcal{R}} \cos(\phi)], \quad (18)$$

$$D = 2\sqrt{\bar{n}_r} \sqrt{\mathcal{T}} \sqrt{\mathcal{R}} \sin(\phi). \quad (19)$$

For the sake of simplicity we have chosen to express the mean photon number for the LO also in units of  $n_o$  by writing  $|\alpha_r|^2 = \bar{n}_r n_o$ .

Notice that  $g^{(2)}(T)$  is independent of the efficiency of detection. This means that it can be measured in counting experiments even when the efficiency of detection is low. For  $T=1$  our results agree with those obtained for the ISHG [10]. For ISHG well below threshold,  $\bar{n}$  is small and  $n_o$  is very large. In this limit  $g^{(2)}(0) \approx (1 - 1/2n_o)^2$ , which is almost unity [10,11].

The expression for  $g^{(2)}(T)$  shows that antibunching arises due to the negative term with coefficient  $C^2$ . It is easy to see that this term is zero or negative, because  $C^2$ ,  $\bar{n}$ ,  $n_o$ , and  $\lambda_1$  are all real and positive. Whenever this term is negative enough to compensate for the positive terms antibunching results. From Eq. (16) the condition for antibunching can be written as

$$C^2 \geq D^2 \left( \frac{\lambda_1}{\lambda_2} \right) + 2T^2 \left( \frac{\gamma \bar{n} \lambda_1}{4n_o} \right) \left( \frac{\lambda_1^2 + \lambda_2^2}{\lambda_1^2 \lambda_1} \right). \quad (20)$$

We find that maximum antibunching occurs for  $\phi = 180^\circ$  for which the coherent component  $A$  reduces to  $(\sqrt{\bar{n}} \sqrt{\mathcal{T}} - \sqrt{\bar{n}_r} \sqrt{\mathcal{R}})^2$ . With a proper choice of the strength of the LO ( $\bar{n}_r n_o = |\alpha_r|^2$ ) and transmissivity ( $=T$ ) we can reduce the coherent component  $A$  considerably, leading to a significant enhancement of antibunching for the HISHG compared to that for the ISHG. In the absence of the coherent component ( $A=0$ ), we find  $C=0$  and the resulting pho-

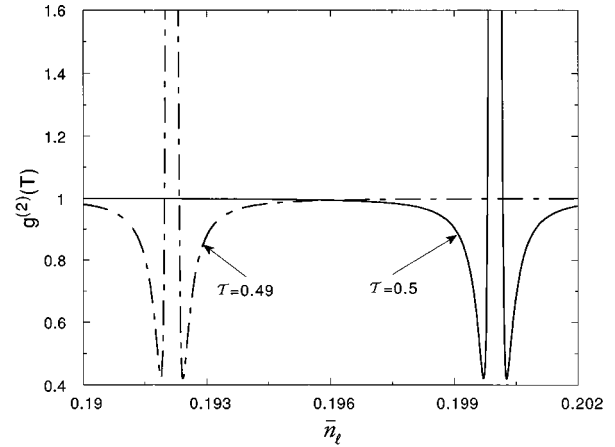


FIG. 2. Normalized second-order intensity correlation function  $g^{(2)}(0)$  for the HISHG as a function of  $\bar{n}_r$  for various parameters  $\bar{n}=0.2$ ,  $n_o=10^6$ ,  $\phi=180^\circ$ , and two different values of transmissivity  $T=0.49$  (dash-dot curve) and  $T=0.5$  (solid curve). Note that  $\bar{n}_r$  is the strength of the LO in units of  $n_o$ . For these parameters  $g^{(2)}(0)$  for the ISHG is indistinguishable from unity.

ton sequence is highly bunched. Thus antibunching is only enhanced when  $A$  is small but not zero.

This behavior of antibunching for the HISHG is shown in Fig. 2, where  $g^{(2)}(0)$  is plotted as a function of  $\bar{n}_r$  for two different values of transmissivity  $T$ . Other parameters are  $n_o=10^6$ ,  $\bar{n}=0.2$ , and  $\phi=180^\circ$ . Note that  $\bar{n}_r$  is the strength of the LO in units of  $n_o$ . Starting from very low values of  $\bar{n}_r$ ,  $g^{(2)}(0)$  decreases as  $\bar{n}_r$  increases, reaching a minimum where antibunching is maximum. With further increase in  $\bar{n}_r$  we find that  $g^{(2)}(0)$  becomes very large, exhibiting a peak for  $\bar{n}_r = \bar{n} T \mathcal{R}$ . This peak corresponds to  $A=0$  and for this figure the peak value is about 51. As we increase  $\bar{n}_r$  further  $g^{(2)}(0)$  decreases, reaching a minimum before reaching the value unity. Thus  $g^{(2)}(0)$  shows two minima as a function

of  $\bar{n}_r$ , where antibunching is enhanced significantly. At these minima the coherent component is partially eliminated by destructive interference at the beam splitter. It is interesting to note that for an antibunched photon sequence a small coherent background is essential. A complete removal of the coherent component results in a highly bunched photon sequence.

Figure 3 shows  $g^{(2)}(0)$  as a function of transmissivity  $T$  for two different values of  $\bar{n}_r$ . Other parameters chosen for this figure are the same as those for Fig. 2. This figure also shows two minima in  $g^{(2)}(0)$  as  $T$  is varied and other parameters are kept constant. At these minima the underlying photon sequence exhibits enhanced antibunching compared to the photon sequence for the ISHG alone.

As mentioned earlier, enhancement of antibunching can also be achieved by using a passive cavity [10,11]. However, for the system under consideration here, one has full control over the strength of the LO, transmittance of the beam splitter, and relative phase. Hence this scheme provides more freedom in accessing the interesting regimes experimentally.

#### IV. MULTIATOM OPTICAL BISTABILITY

Next we consider the enhancement of antibunching in the MAOB, in which  $N$  two-level atoms are placed inside a

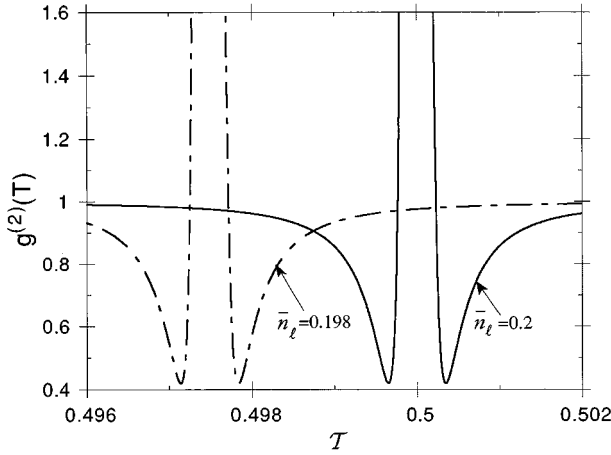


FIG. 3. Normalized second-order intensity correlation function  $g^{(2)}(0)$  for the HISHG as a function of transmissivity  $T$  for various parameters  $\bar{n}=0.2$ ,  $n_o=10^6$ ,  $\phi=180^\circ$ , and two different values of  $\bar{n}_l=0.198$  (dash-dot curve) and  $=0.2$  (solid curve). For these parameters  $g^{(2)}(0)$  for the ISHG is indistinguishable from unity.

high- $Q$  cavity. The cavity is driven by a strong coherent field of amplitude  $E$  which again can be chosen to be real by an appropriate definition of phases. In the positive- $P$  representation the relevant quantum operators can be mapped onto five stochastic variables: three describing atomic dynamics and two describing cavity-field dynamics [11]: In the good cavity limit atomic variables decay much faster than the field variables. They can therefore be eliminated adiabatically. In this limit cavity-field variables satisfy the following differential equations [11]:

$$\dot{\alpha}_s = -\gamma(\alpha_s - E) - 2C\gamma\alpha_s + i\sqrt{2C\gamma}\alpha_s\xi, \quad (21)$$

$$\dot{\alpha}_{s*} = -\gamma(\alpha_{s*} - E) - 2C\gamma\alpha_{s*} + i\sqrt{2C\gamma}\alpha_{s*}\xi_*, \quad (22)$$

Here  $\gamma$  is the cavity decay rate;  $C=(N\gamma_\perp)/(n_o\gamma)$  is the atomic cooperativity parameter;  $n_o=(2\gamma_\perp\gamma_\parallel)/(4g^2)$  is the saturation photon number;  $\gamma_\perp$  is the atomic dipole dephasing rate;  $\gamma_\parallel$  is the population decay rate;  $g$  is the atom-field coupling constant;  $\xi$  and  $\xi_*$  are two real Gaussian white-noise processes with zero mean and unit strength. Linearizing  $\alpha_s$  and  $\alpha_{s*}$  around the steady-state values

$$\alpha_s = \sqrt{n_o}[\sqrt{\bar{n}} + i\delta\alpha_s], \quad (23)$$

$$\alpha_{s*} = \sqrt{n_o}[\sqrt{\bar{n}} + i\delta\alpha_{s*}], \quad (24)$$

one can show that  $\delta\alpha_s$  and  $\delta\alpha_{s*}$  satisfy the following differential equations:

$$\dot{\delta\alpha}_s = -\lambda\delta\alpha_s + \sqrt{\frac{2C\gamma\bar{n}}{n_o}}q_1, \quad (25)$$

$$\dot{\delta\alpha}_{s*} = -\lambda\delta\alpha_{s*} + \sqrt{\frac{2C\gamma\bar{n}}{n_o}}q_2, \quad (26)$$

with  $\lambda = \gamma(1+2C)$ . Here  $\bar{n}$  is average photon number in the fundamental mode given by  $\bar{n}n_o(1+2C)^2 = E^2$ . Using Eqs.

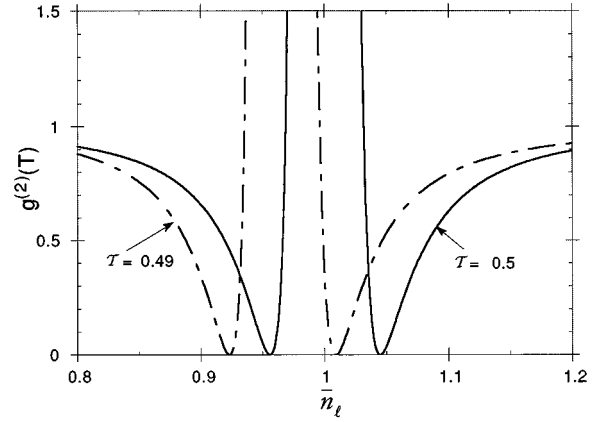


FIG. 4. Normalized second-order intensity correlation function  $g^{(2)}(0)$  for the HMAOB as a function of  $\bar{n}_l$  for various parameters  $\bar{n}=1$ ,  $n_o=10^3$ ,  $C=50$ ,  $\phi=180^\circ$ , and two different values of transmissivity  $T=0.49$  (dash-dot curve) and  $T=0.5$  (dash-dot curve). For these parameters  $g^{(2)}(0)$  for the MAOB is indistinguishable from unity.

(25) and (26) one can show that  $\delta\alpha_s$  and  $\delta\alpha_{s*}$  have zero mean and correlation functions given by

$$\langle \delta\alpha_s(t)\delta\alpha_s(t') \rangle = \frac{\bar{n}}{2n_s} e^{-\lambda|t-t'|} = \langle \delta\alpha_{s*}(t)\delta\alpha_{s*}(t') \rangle, \quad (27)$$

$$\langle \delta\alpha_{s*}(t)\delta\alpha_s(t') \rangle = 0, \quad (28)$$

with  $n_s = n_o(1+2C)/(2C)$ .

Substituting  $\alpha_s$  and  $\alpha_{s*}$  into Eqs. (2) and (3) we get complex-field amplitudes for the HMAOB as

$$\beta_1 = \sqrt{n_o}[\sqrt{\bar{n}} + i\delta\alpha_s]\sqrt{T} + |\alpha_l|e^{i\phi}\sqrt{\mathcal{R}}, \quad (29)$$

$$\beta_{1*} = \sqrt{n_o}[\sqrt{\bar{n}} + i\delta\alpha_{s*}]\sqrt{T} + |\alpha_l|e^{-i\phi}\sqrt{\mathcal{R}}. \quad (30)$$

Using the correlation properties of  $\delta\alpha_s$  and  $\delta\alpha_{s*}$  we obtain the following expressions for the mean and the two-time intensity correlation function:

$$\langle \beta_{1*}\beta_1 \rangle = n_o[A], \quad (31)$$

$$g^{(2)}(T) = 1 + \frac{[\bar{n}^2 T^2 e^{-2\lambda T} - 4\bar{n}n_s T F e^{-\lambda T}]}{[2n_s A]^2}, \quad (32)$$

where  $A$  is given by Eq. (17), and  $F$  is given by

$$F = \bar{n}T + \bar{n}_l \mathcal{R} \cos(2\phi) + 2\sqrt{\bar{n}}\sqrt{\bar{n}_l}\sqrt{T}\sqrt{\mathcal{R}} \cos(\phi). \quad (33)$$

Here  $\bar{n}_l$  is the mean photon number for the LO in units of  $n_o$ . For  $T=1$ , the results for the HMAOB reduce to those for the MAOB. For the MAOB  $g^{(2)}(0) = (1-1/2n_s)^2$ , which is almost 1 for a large value of  $n_s$  [11].

The behavior of  $g^{(2)}(T)$  for the HMAOB is similar to that for the HISHG. As in the case of HISHG we find that maximum antibunching for the HMAOB occurs at  $\phi=180^\circ$  and antibunching is enhanced by reducing the coherent background  $A$  by adjusting the parameters  $\bar{n}_l$  and  $T$ .

Figure 4 shows  $g^{(2)}(0)$  as a function of  $\bar{n}_l$  for two dif-

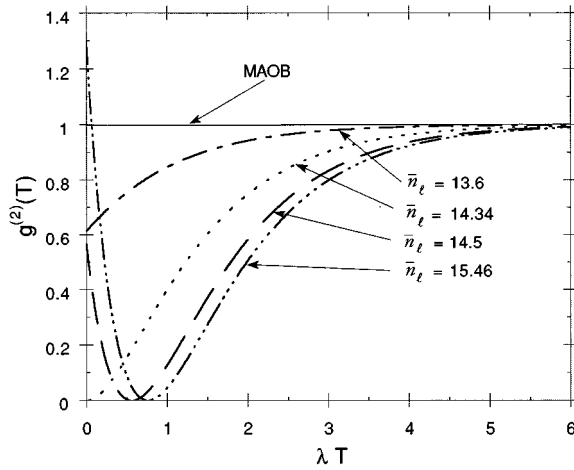


FIG. 5. Normalized second-order intensity correlation function  $g^{(2)}(T)$  for the HMAOB as a function of  $\lambda T$  for parameters  $\bar{n}=5$ ,  $n_o=10^3$ ,  $\mathcal{C}=50$ ,  $T=0.75$ , and  $\phi=180^\circ$ . Curves are plotted for different values of  $\bar{n}_r$ : 13.6 (dash-dot curve), 14.34 (dotted curve), 14.5 (dashed curve), and 15.46 (— · — · — · —). These dash-dot curves show enhancement of antibunching and violation of the classical inequality  $g^{(2)}(0) \geq 1$ . The curve for  $\bar{n}_r=15.46$  shows violation of the classical inequality  $[g^{(2)}(0)-1] \geq |g^{(2)}(T)-1|$ . The solid curve for the MAOB is indistinguishable from unity for all values of  $\lambda T$ .

ferent values of parameter  $\mathcal{T}$  and  $\phi=180^\circ$ . Once again, as a function of  $\bar{n}_r$ , we find  $g^{(2)}(0)$  shows two minima where it approaches zero. At these two minima the underlying photon sequence exhibits maximum antibunching. This enhancement in antibunching occurs due to destructive interference at the beam splitter.

Figure 5 shows  $g^{(2)}(T)$  as a function of scaled time  $\lambda T$  for  $\mathcal{T}=3/4$ ,  $\phi=180^\circ$ , and several different values of  $\bar{n}_r$ . Depending on the value of  $\bar{n}_r$  we find that the photon sequence at the output port is bunched [ $g^{(2)}(0) > 1$ ] or antibunched [ $g^{(2)}(0) < 1$ ]. For  $\bar{n}_r=13.6$  (dash-dot curve),  $\bar{n}_r=14.34$  (dotted curve), and  $\bar{n}_r=14.5$  (dashed curve) antibunching is enhanced. For the dash-dot curve  $g^{(2)}(T)$  monotonically increases to unity as  $T$  increases, whereas the dashed curve shows a minimum at a nonzero time. For  $\bar{n}_r=14.34$  (dotted curve)  $g^{(2)}(0)$  is nearly zero, indicating perfect antibunching. The curves for  $\bar{n}_r=13.6$  and  $\bar{n}_r=14.34$  have a positive slope at time  $T=0$ , whereas those for  $\bar{n}_r=14.5$  and  $\bar{n}_r=15.46$  have a negative slope at time  $T=0$ . Even though the curves  $\bar{n}_r=13.6$

and  $\bar{n}_r=14.34$  have a positive slope at  $T=0$ , this positive slope does not reflect a new violation of inequality, because  $g^{(2)}(0) < 1$  implies that  $g^{(2)}(0) < g^{(2)}(T)$ .

An interesting case is shown by the curve for  $\bar{n}_r=15.46$ . In this case we find that  $g^{(2)}(0) (=1.29)$  is greater than unity. This corresponds to a bunched photon sequence. We note that  $g^{(2)}(0)$  is also greater than  $g^{(2)}(T)$ . This curve shows an interesting violation of the classical inequality [19,13]

$$g^{(2)}(0) - 1 \geq |g^{(2)}(T) - 1|. \quad (34)$$

From this inequality it follows that if  $1 \leq g^{(2)}(0) \leq 2$ , then  $g^{(2)}(T)$  cannot fall below  $[2 - g^{(2)}(0)] (=0.71)$  for a classical field. Since  $g^{(2)}(T)$  falls below this value this classical inequality is violated. A similar feature appears in the light transmitted from a driven two-level atom [19] and homodyne detection of degenerate parametric oscillator [13]. It is interesting to note that the minimum in the  $g^{(2)}(T)$  occurs at a time of the order of  $(\lambda)^{-1}$ . This means that for these parameters, the probability of detecting two photons separated by  $\lambda T$  is negligible.

## V. SUMMARY AND CONCLUSIONS

We have discussed enhancement of antibunching in the ISHG and the MAOB. The scheme presented here is based on homodyne detection in which a signal from the ISHG or the MAOB is mixed with a coherent local oscillator at a lossless beam splitter.

We have shown that by choosing the strength of the LO, transmittance of the beam splitter, and relative phase between the signal and the LO we can enhance antibunching of the homodyne field significantly. The enhancement of antibunching is due to the *partial* removal of coherent background by destructive interference at the beam splitter. For an antibunched photon sequence a small coherent component is essential, and in the absence of a coherent component a highly bunched photon sequence is generated. We also find that the homodyne field may be bunched but it can exhibit a violation of the classical inequality  $g^{(2)}(0) - 1 \geq |g^{(2)}(T) - 1|$ .

## ACKNOWLEDGMENT

This work was supported in part by the National Science Foundation.

- [1] See the special issue on *Squeezed States of the Electromagnetic Field*, edited by H. J. Kimble and D. F. Walls, *JOSA B* **4**, (10), (1987); L. Wu, H. J. Kimble, J. L. Hall, and H. Wu, *Phys. Rev. Lett.* **57**, 2520 (1986); P. W. Milonni and S. Singh, in *Advances in Atomic, Molecular, and Optical Physics*, edited by D. Bateman and B. Bederson (Academic, Orlando, FL, 1991), Vol. 28, p. 75.
- [2] H. J. Carmichael and D. F. Walls, *J. Phys. B* **9**, L43 (1976); H. J. Kimble and L. Mandel, *Phys. Rev. A* **13**, 2123 (1976).

- [3] H. J. Kimble, M. Dagenais, and L. Mandel, *Phys. Rev. Lett.* **38**, 691 (1977); G. Rempe, F. Schmidt-Kaler, and H. Walther, *ibid.* **64**, 2783 (1990).
- [4] L. Mandel, *Phys. Rev. Lett.* **49**, 136 (1982).
- [5] R. Loudon, *Rep. Prog. Phys.* **43**, 913 (1980); H. Paul, *Rev. Mod. Phys.* **54**, 1061 (1982).
- [6] P. D. Drummond, K. J. McNeil, and D. F. Walls, *Opt. Acta* **27**, 321 (1980); **28**, 211 (1981).
- [7] P. D. Drummond and D. F. Walls, *J. Phys. A* **13**, 725 (1980); H.

- J. Carmichael, D. F. Walls, P. D. Drummond, and S. S. Hassan, *Phys. Rev. A* **27**, 3112 (1983).
- [8] H. J. Carmichael, *Phys. Rev. Lett.* **55**, 2790 (1985); *Phys. Rev. A* **33**, 3262 (1985); H. J. Carmichael, J. S. Satchell, and S. Sarker, *ibid.* **34**, 3166 (1986).
- [9] A. Bandilla and H. H. Ritze, *Opt. Commun.* **28**, 126 (1979); H. H. Ritze and A. Bandilla, *ibid.* **28**, 241 (1979).
- [10] G. S. Holliday and Surendra Singh, in *Coherence and Quantum Optics VI*, edited by J. H. Eberly, L. Mandel, and E. Wolf (Plenum, New York, 1990), p. 509.
- [11] Y. Qu, M. Xiao, G. S. Holliday, S. Singh, and H. J. Kimble, *Phys. Rev. A* **45**, 4932 (1992), and references therein.
- [12] M. Xiao and H. J. Kimble, *J. Opt. Soc. Am. A* **3**, 46 (1986).
- [13] A. B. Dodson and Reeta Vyas, *Phys. Rev. A* **47**, 3396 (1993).
- [14] R. A. Campos, B. E. A. Saleh, and M. C. Teich, *Phys. Rev. A* **40**, 1371 (1989).
- [15] S. L. Braunstein, *Phys. Rev. A* **42**, 474 (1990); S. L. Braunstein and C. M. Caves, **42**, 4115 (1990).
- [16] Reeta Vyas and S. Singh, *Phys. Rev. A* **38**, 2423 (1988); *Opt. Lett.* **14**, 1110 (1989); *Phys. Rev. A* **40**, 5147 (1989); R. Vyas and A. L. DeBrito, *ibid.* **42**, 592 (1990).
- [17] G. S. Agarwal and G. Adam, *Phys. Rev. A* **39**, 6259 (1989); M. J. Wolinsky and H. J. Carmichael, in *Coherence and Quantum Optics VI*, edited by J. H. Eberly, L. Mandel, and E. Wolf (Plenum, New York, 1989); C. Zhu and C. M. Caves, *Phys. Rev. A* **42**, 6794 (1990).
- [18] P. D. Drummond and C. W. Gardiner, *J. Phys. A* **13**, 2353 (1980).
- [19] P. Rice and H. J. Carmichael, *IEEE J. Quantum Electron.* **JQE-24**, 1351 (1988).
- [20] R. Loudon, *The Quantum Theory of Light* (Oxford Science Publications, Oxford, 1983).
- [21] C. W. Gardiner, *Handbook of Stochastic Methods* (Springer-Verlag, Berlin, 1983).
- [22] H. Risken, *The Fokker-Planck Equation* (Springer-Verlag, Berlin, 1984).